Electronic Supplementary Material (ESI) for Journal of Materials Chemistry A.

Supplementary Information

Structural transition in orthorhombic $Li_{5-x}H_xLa_3Nb_2O_{12}$ garnets induced by a concerted lithium and proton diffusion mechanism

María Luisa Sanjuán,[1] Alodia Orera,[1] Isabel Sobrados,[2] Antonio F. Fuentes,[3] and Jesús Sanz[2]*

[1]Instituto de Ciencia de Materiales de Aragón (CSIC - Universidad de Zaragoza), Facultad de Ciencias, Universidad de Zaragoza, 50009 Zaragoza, Spain

[2]Instituto de Ciencia de Materiales de Madrid (CSIC), Cantoblanco, 28049 Madrid, Spain

[3]Cinvestav Unidad Saltillo, Apartado Postal 663, 25000 Saltillo, Coahuila, México

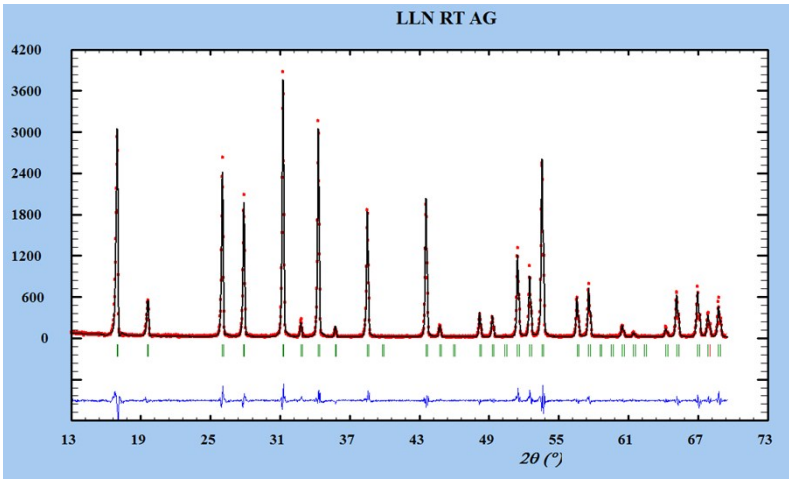

Fig. S1: Profile fit of the PXRD pattern of as-prepared $Li_5La_3Nb_2O_{12}$ with S.G. Ia-3d (230), a=12.7967(3) Å.

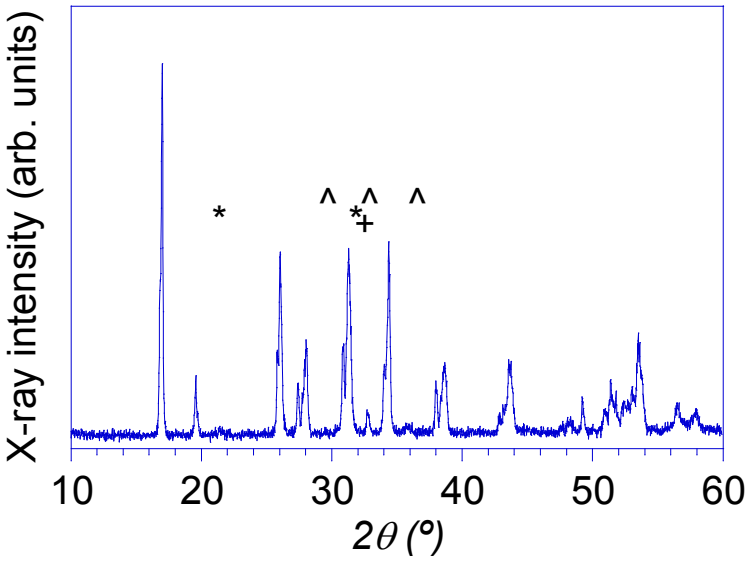

Fig. S2: XRD pattern of as-aged LLNO. The main peaks of possible Li-containing second phases are indicated with ^ ($LiOH.H_2O$), + (LiOH) and * (Li_2CO_3).

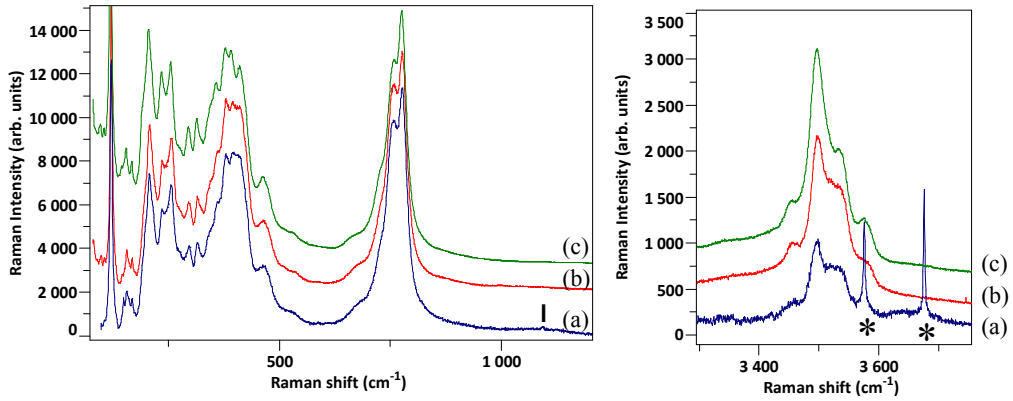

Fig. S3. Raman spectra of aged LLNO after successive preparation steps: (a) as aged; (b) after washing and (c) after 1h homogenization at 200 °C. The non-washed sample presents strong $LiOH.H_2O$ and LiOH bands (3575 and 3675 cm^{-1}, resp., marked with *), as well as a weak peak from Li_2CO_3 at 1093 cm^{-1} (marked with a bar). Washing suppresses these secondary phases without affecting the bands from the garnet phase (see section 3.4.1). The short annealing at 200 °C sharpens the bands and increases spectral resolution.

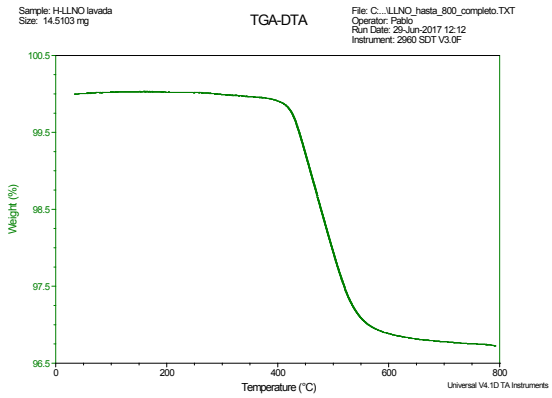

Fig. S4: TG curve of aged $Li_5La_3Nb_2O_{12}$ after washing in distilled water to remove second-phases.

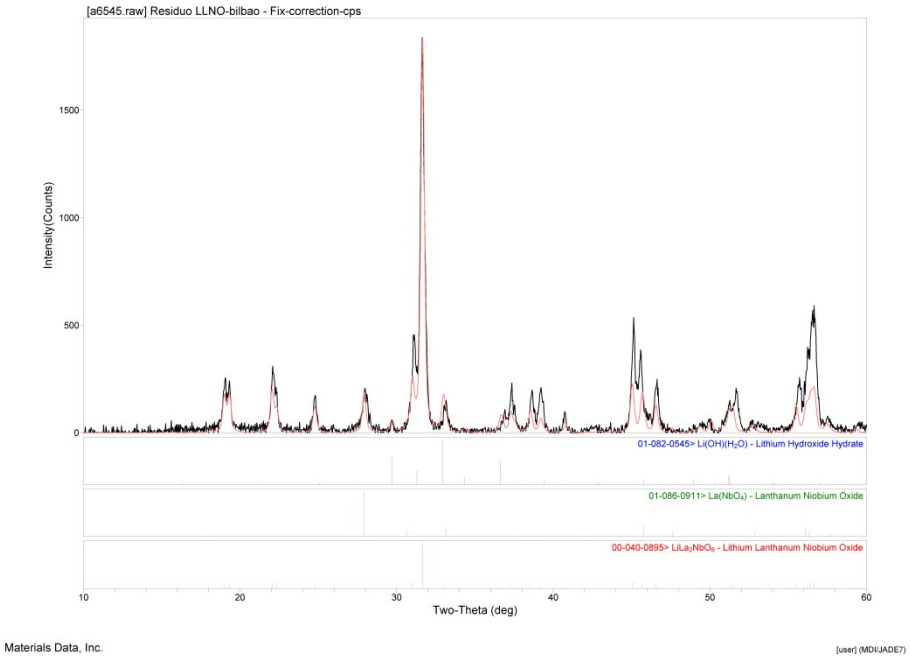

Fig. S5: XRD pattern and phase assignment of the TG residue of H-LLNO after 800 °C showing $LiLa_2NbO_6$ and $LaNbO_4$ as the main decomposition phases.

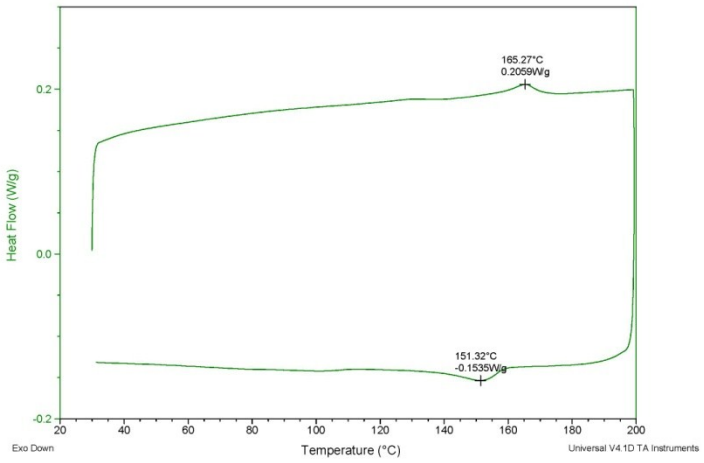

Fig. S6: DSC curve of H-LLNO between RT and 200 °C, displaying an endothermic event at 165 °C on heating and an exothermic one at 151 °C on cooling.

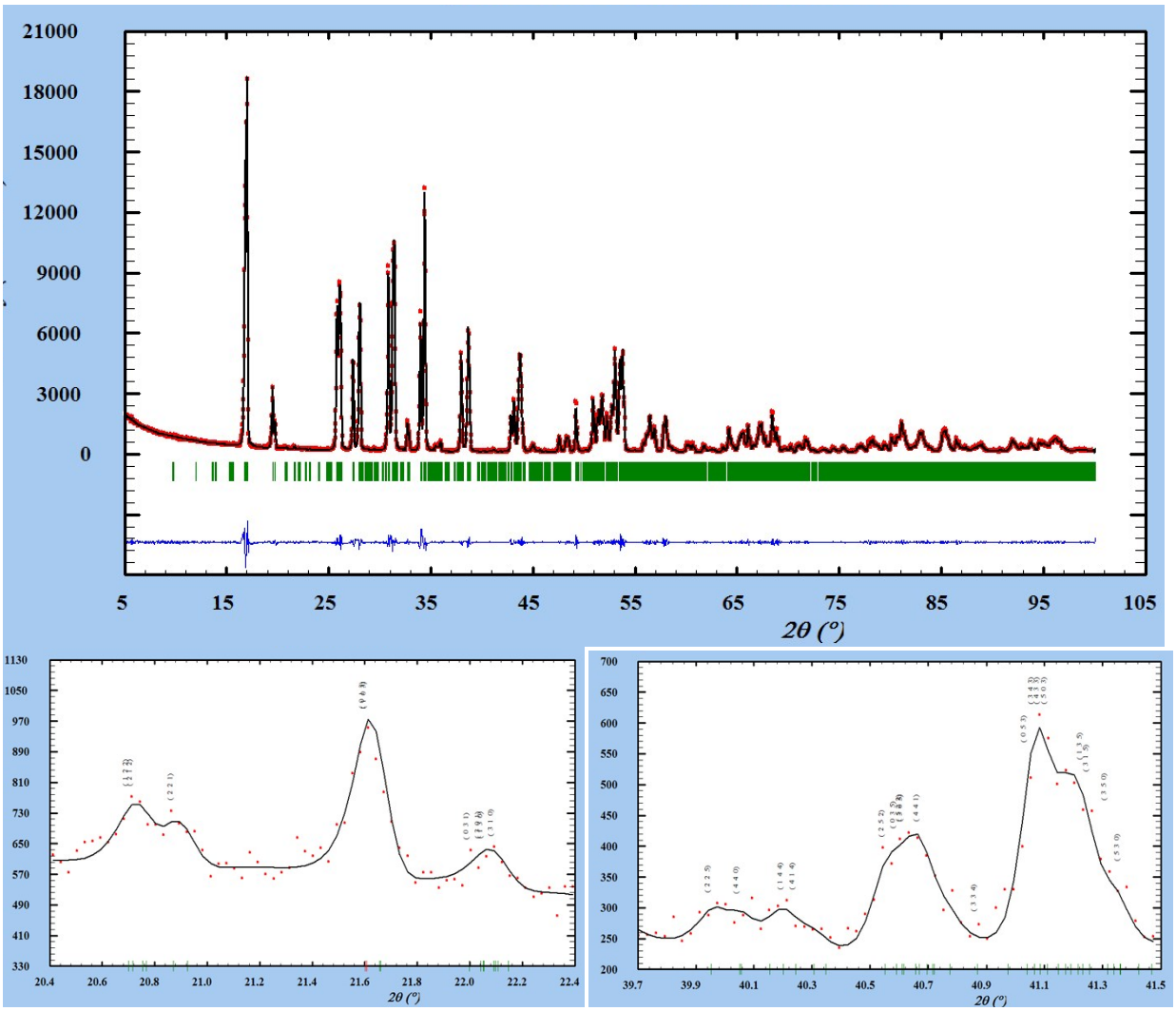

Fig. S7. Profile fit of the RT XRD pattern (t=3s, above) in the $P2_12_12_1$ (#19) SG and selected regions measured with t=6s showing low intensity reflections (below).

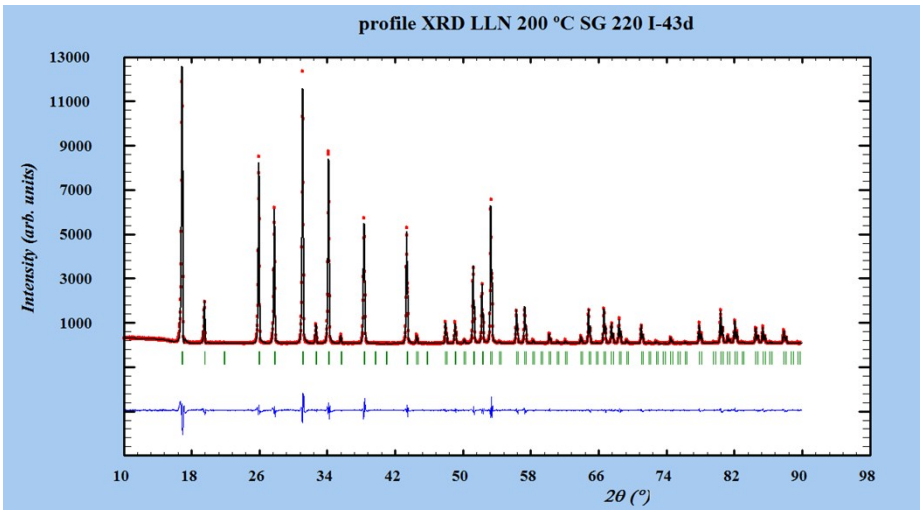

Fig. S8. Profile fit of the XRD pattern at 200 °C in the *I*-43*d* (#220) SG. X^2: 3.60.

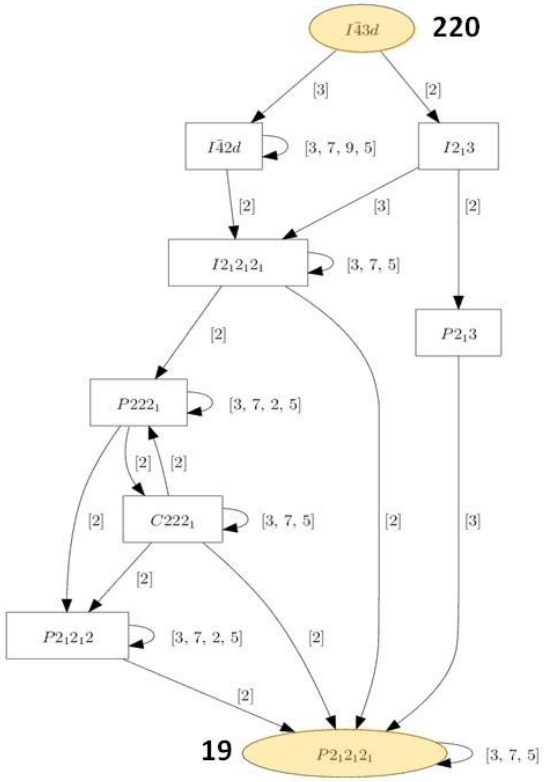

Fig. S9: Tree depicting the relation between the SGs of the high and low temperature phases of H-LLNO (*I*-43*d* and $P2_12_12_1$, respectively). Adapted from the Bilbao Crystallographic Server (ref. 23 in the main text).

Table S1

Relevant bond-distances in the low-temperature phase of H-LLNO derived from the fit of the RT PND in the $P2_12_12_1$ SG.

La1 - O1 : 2.47
La1 - O3 : 2.58
La1 - O10 : 2.54
La1 - O11 : 2.51
La1 - O13 : 2. 55
La1 – O15 : 2.51
La1 – O22: 2.66
La1 – O23 : 2.58

La2 - O1 : 2.44
La2 - O2 : 2.50
La2 - O10 : 2.50
La2 - O12 : 2.63
La2 - O13 : 2.71
La2 – O14: 2.58
La2 – O22 : 2.43
La2 – O24 : 2.54

La3 - O2 : 2.52
La3 - O3 : 2.40
La3 - O11 : 2.59
La3 - O12 : 2.51
La3 – O14 : 2.57
La3 – O15: 2.47
La3 – O23 : 2.54
La3 – O24: 2.42

La4 - O4 : 2.50
La4 - O6 : 2.68
La4 - O7 : 2.63
La4 - O8 : 2.54
La4 – O16 : 2.45
La4 – O18: 2.40
La4 – O19: 2.46
La4 – O20: 2.45

La5 - O4 : 2.74
La5 - O5 : 2.54
La5 - O7 : 2.55
La5 - O9 : 2.63
La5 – O16 : 2.44
La5 – O17: 2.45
La5 – O19: 2.48
La5 – O21: 2.44

La6 - O5 : 2.56
La6 - O6 : 2.48
La6 - O8 : 2.47
La6 - O9 : 2.41
La6 – O17 : 2.66
La6 – O18: 2.54
La6 – O20: 2.67
La6 – O21: 2.51

Nb1 – O10 : 2.11
Nb1 – O11: 2.31
Nb1 – O12: 1.98
Nb1 - O16 : 1.81
Nb1 - O17 : 1.84
Nb1 - O18 : 1.89

Nb2 - O1 : 1.84
Nb2 - O2 : 1.84
Nb2 - O3 : 2.02
Nb2 – O19 : 2.23
Nb2 – O20: 2.17
Nb2 – O21: 1.97

Nb3 – O4 : 1.90
Nb3 – O5 : 1.92
Nb3 – O6 : 2.05
Nb3 – O22 : 2.13
Nb3 – O23: 2.15
Nb3 – O24: 1.87

Nb4 – O7 : 2.16
Nb4 – O8 : 2.13

Nb4 – O9 : 1.97
Nb4 – O13 : 1.91
Nb4 – O14: 1.87
Nb4 – O15 : 1.97

Li1 - O1 : 1.824
Li1 - O5 : 1.93
Li1 - O13 : 1.90
Li1 – O17 : 2.10

Li2 - O2 : 1.87
Li2 - O4 : 2.19
Li2 – O14 : 2.02
Li2 – O16: 1.95

Li3 - O3 : 1.94
Li3 - O6 : 1. 87
Li3 – O15 : 2.06
Li3 – O18 : 2.06

Li4 - O7 : 2.00
Li4 - O11 : 1.80
Li4 – O19 : 1.96
Li4 – O23 : 1.83

Li5 - O8 : 1.98
Li5 - O10 : 1.80
Li5 – O20 : 2.14
Li5 – O22 : 1.89

Li6 - O9 : 2.01
Li6 - O12 : 1.96
Li6 – O21 : 2.00
Li6 – O24: 2.19

H1 - O8 : 1.02
H2 - O23 : 0.98
H3 - O10: 1.03
H4 - O20: 1.17
H5 - O11 : 1.03
H6 - O22 : 1.10
H7 - O7 : 0.92
H8 - O19: 0.90

H1 - H3 : 1.51
H1 - H4 : 2.77
H1 - H6 : 2.69
H3 - H4 : 2.30
H3 - H6 : 3.44

H2 - H5 : 2.41
H2 - H7 : 1.88
H2 - H8 : 1.89
H5 - H7 : 1.76
H5 - H8 : 2.04

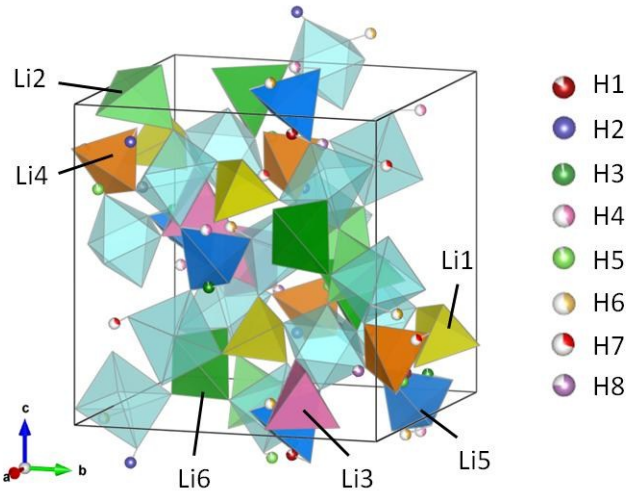

Fig. S10. Unit cell resulting from fitting the RT PND pattern with the $P2_12_12_1$ SG. Atom coordinates and occupancies are given in Table 1 of the main text**.**

Table S2. Relevant distances in the high temperature phase of H-LLNO derived from the fit of the 200 °C PND in the *I*-43*d* SG.

La1 - O1 : 2.57 x2
La1 - O1 : 2.56 x2
La1 - O2 : 2.44 x2
La1 - O2 : 2.58 x2

Nb1 - O1 : 2.07 x3
Nb1 - O2 : 1.94 x3

Li1(12b) - O1 : 1.93 x4
Li2(12a) - O2 : 1.99 x4

Li3 - O1 : 2.28
Li3 - O1 : 1.82
Li3 - O1 : 2.43
Li3 - O2 : 2.51
Li3 - O2 : 2.61
Li3 - O2 : 2.11

H1 - O1 : 0.94

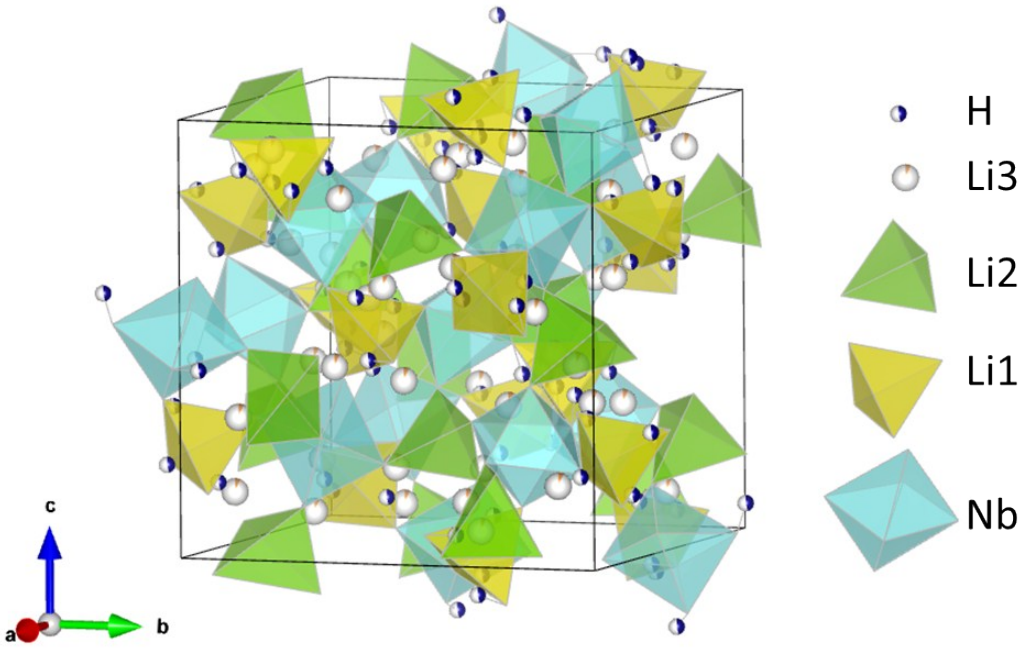

Fig. S11. Unit cell of the high temperature phase (*I*-43*d* SG), showing Li1 and Li2 tetrahedra, Nb octahedra and H bonding to Li1 tetrahedra. Large spheres represent octahedral Li ions (Li3).

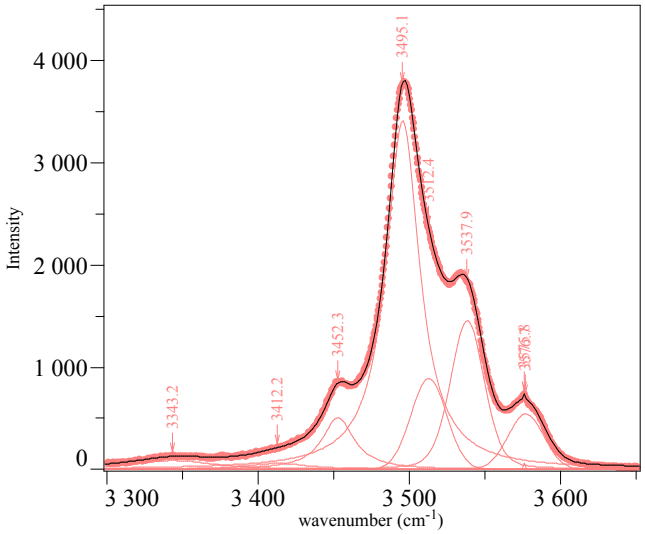

Fig. S12. Profile decomposition of the OH^- stretching region of the RT Raman spectrum.

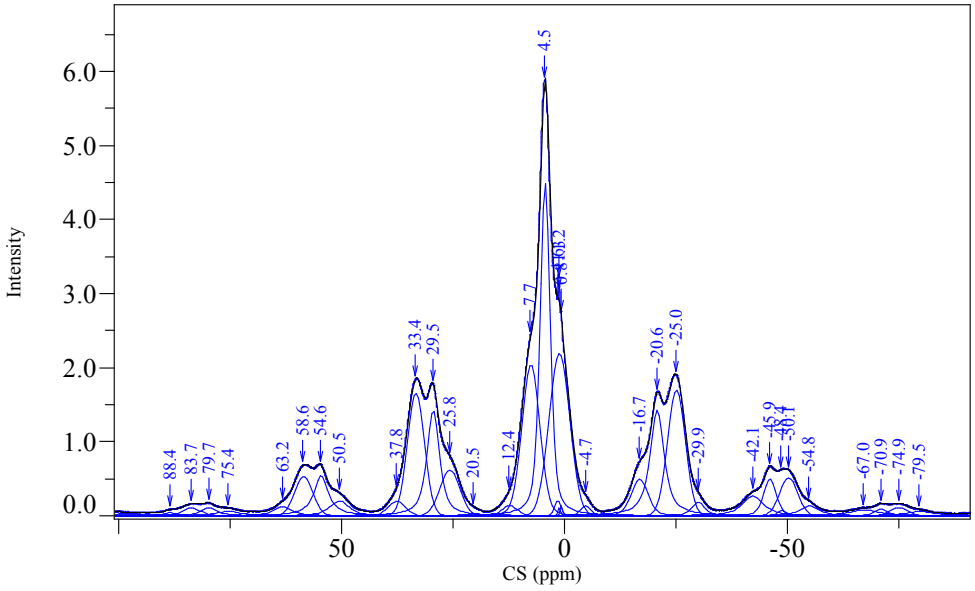

Fig. S13. Profile decomposition of the ^1H MAS-NMR spectrum (ν_r = 10 KHz).